



Review

# Plant-Biomass-Derived Carbon Materials as Catalyst Support, A Brief Review

Antonina A. Stepacheva <sup>\*</sup>, Mariia E. Markova, Yury V. Lugovoy, Yury Yu. Kosivtsov, Valentina G. Matveeva   
and Mikhail G. Sulman

Department of Biotechnology, Chemistry and Standardization, Tver State Technical University,  
A. Nikitin Str., 22, 170026 Tver, Russia

\* Correspondence: a.a.stepacheva@mail.ru; Tel.: +7-(4822)789348

**Abstract:** Carbon materials are widely used in catalysis as effective catalyst supports. Carbon supports can be produced from coal, organic precursors, biomass, and polymer wastes. Biomass is one of the promising sources used to produce carbon-based materials with a high surface area and a hierarchical structure. In this review, we briefly discuss the methods of biomass-derived carbon supported catalyst preparation and their application in biodiesel production, organic synthesis reactions, and electrocatalysis.

**Keywords:** plant biomass; carbon; biochar; catalysts

## 1. Introduction

Carbon materials, such as graphite, graphene, activated carbon, carbon nanotubes (CNT), nanosheets (CNS), and nanofibers (CNF), are widely used in catalysis. Such materials are considered to be promising catalytic supports because of their high specific surface area, resistance to acidic or basic media, amphoteric character, high-temperature stability, tailored pore size distribution, ability for modification, and cheapness [1–3]. Carbon supports can be produced from coal, organic precursors, biomass, and polymer waste through different techniques, which are mainly based on thermochemical degradation/decomposition methods. In recent years, biomass-derived carbonaceous materials have attracted great attention due to their cheapness, simple preparation, and wide range of biomass resources.

To produce carbon materials from biomass, different thermochemical methods can be used. Among them, four main techniques are highlighted (Figure 1). Combustion of biomass is widely used to obtain ashes that are characterized by the contents of alkali and alkali-earth metal compounds with a low content of carbon (1–15 wt.%). Depending on the biomass type, the resulting ashes have different elemental compositions, varying from 10–50 wt.% of alkali metals, 5–20 wt.% of alkali-earth metals, 0.5–2 wt.% of Al, 2–80 wt.% of Si, and 0.5–10 wt.% of Cl, P, Mn, Fe, Zn, etc. [4]. The calcination method is carried out in a wide temperature range from 300 to 1000 °C [5]. Calcination can be performed either in the air or in an inert atmosphere, resulting in the degradation of biomass components to form carbon and inorganic compounds, such as alkali and alkali-earth metal carbonates and carbides. During calcination, temperature and biomass retention time play a critical role in the formation of the resulting carbon material morphology and structure. It is reported that a high reaction temperature and a short retention time lead to the aggregation of particles of Ca, Na, Mg, and Si oxides and, thus, reduce the specific surface area and porosity of the resulting catalysts [6,7]. Despite the simplicity of the combustion and calcination methods, the resulting materials have a low specific surface area, poor porosity, and low carbon content, leading to their limited application in catalysis.



**Citation:** Stepacheva, A.A.; Markova, M.E.; Lugovoy, Y.V.; Kosivtsov, Y.Y.; Matveeva, V.G.; Sulman, M.G.

Plant-Biomass-Derived Carbon Materials as Catalyst Support, A Brief Review. *Catalysts* **2023**, *13*, 655.  
<https://doi.org/10.3390/catal13040655>

Academic Editor: Jaroslaw Polanski

Received: 10 February 2023

Revised: 17 March 2023

Accepted: 24 March 2023

Published: 27 March 2023



**Copyright:** © 2023 by the authors. Licensee MDPI, Basel, Switzerland. This article is an open access article distributed under the terms and conditions of the Creative Commons Attribution (CC BY) license (<https://creativecommons.org/licenses/by/4.0/>).

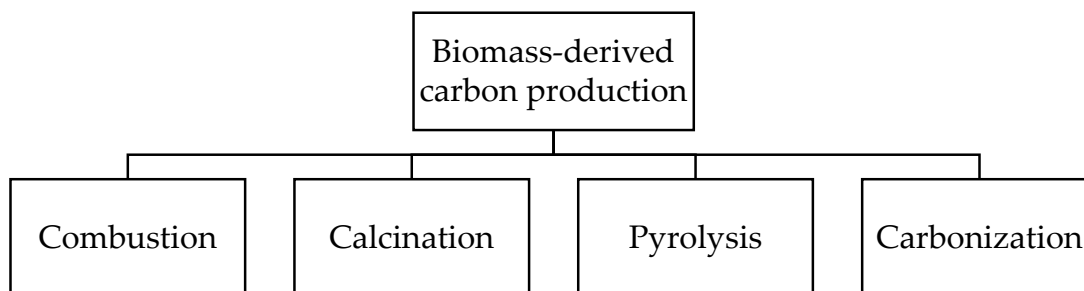


**Figure 1.** Main methods for biomass-derived carbon production.

Another two methods are used to prepare biochar characterized by a high porosity with a hierarchical structure. Pyrolysis is a widely used method to obtain biochar from organogenic feedstock. Depending on the temperature and the feedstock residence time, pyrolysis can be divided into slow pyrolysis occurring at 300–700 °C for several hours [8,9] and fast pyrolysis performed at 500–1000 °C at a residence time <10 s [10]. Typically, slow pyrolysis results in a biochar yield ranging from 30 to 70 wt.%, while the fast process provides a biochar yield of up to 15 wt.% [9]. Besides conventional non-catalytic pyrolysis to provide biochar production, biomass feedstock can be preliminarily treated with a metal salt solution (catalytic pyrolysis), which leads to the formation of metal-containing composites. The carbonization method seems to be close to pyrolysis and consists of heating biomass in an inert atmosphere (N<sub>2</sub> or Ar) at relatively low temperatures. This method can be divided into two types depending on the media used. Dry carbonization is carried out at 300–600 °C using dried feedstock [11]. Wet or hydrothermal carbonization (HTC) is performed in superheated water using either dried or wet feedstock at a temperature of 180–800 °C [12]. The latter can be classified into high-temperature (300–800 °C) and low-temperature (180–250 °C) HTC [13–15]. The high-temperature process results in the formation of carbon materials with a high surface area and a high porosity, with a hierarchical structure, while the low-temperature HTC is used for the production of colloidal carbonaceous spheres [15].

Moreover, techniques such as gasification and torrefaction can be mentioned for biochar production. Gasification is the process mainly used for synthesis gas production from biomass occurring at a temperature of 750–900 °C. Meanwhile, about 10 wt.% of biochar can be obtained by gasification [16]. Torrefaction is direct carbonization of biomass at low temperatures (up to 250–300 °C), resulting in over 80 wt.% of biochar formation [17]. The composition, structure, morphology, and textural properties of carbon materials strongly depend on the biomass type, the preparation method used, the temperature, the size of the particle, the heating rate, the residence time, etc.

Despite the different production methods, biomass-derived carbon materials find a wide range of application in catalysis. Four main directions can be highlighted: biodiesel production, organic reactions, electrocatalysis, and photocatalysis. In this review, we briefly discuss the first three directions for the use of biomass-derived carbon-based catalysts.

## 2. Biomass-Derived Carbon-Based Catalysts for Biodiesel Production

In recent years, biomass-carbon-based catalysts are widely used in esterification/trans-esterification processes to produce fatty acid methyl esters (FAMES). Carbon produced via pyrolysis, calcination, or carbonization tends to be functionalized by sulfonic groups or alkali to form acidic or basic active sites (Figure 2). Two directions for the functionalization are used: (i) direct functionalization through the introduction of functional groups into the raw material, and (ii) post-synthesis modification through the treatment of carbonaceous materials [15].

### 2.1. Acid-Functionalized Catalysts

Acidic carbon-based catalysts are efficiently applied in esterification/transesterification processes. The most widely used ones are sulfonated carbons characterized by a high acid density. These catalysts can substitute concentrated sulfuric acid in many reactions, including biodiesel production [18]. Sulfonated catalysts are synthesized by either direct sulfonation with  $H_2SO_4$  or by sulfonation via reductive alkylation. In contrast to concentrated sulfuric acid, carbon-based catalysts tend to cause less corrosion and can be easily separated from the reaction mixture.

A review of recent works on sulfonated carbon catalysts shows that these catalysts, regardless of the method of preparation, are consisted of amorphous or graphite-like carbon with covalently bonded  $-SO_3H$  groups. The last ones provide the Brønsted acid sites with a high density. The surface area of the resulting composites mainly depends on the carbon preparation method. These catalysts have a high activity in the production of biodiesel from feedstock with high free fatty acid (HFFA) content [19,20]. Incomplete carbonization of the biomass raw material during the catalyst synthesis leads to the formation of a polycyclic carbon-ring structure with  $-COOH$  or  $-OH$  groups on the surface, which increases the catalyst acidity and facilitates the covalent bonding of sulfonic groups [21,22].

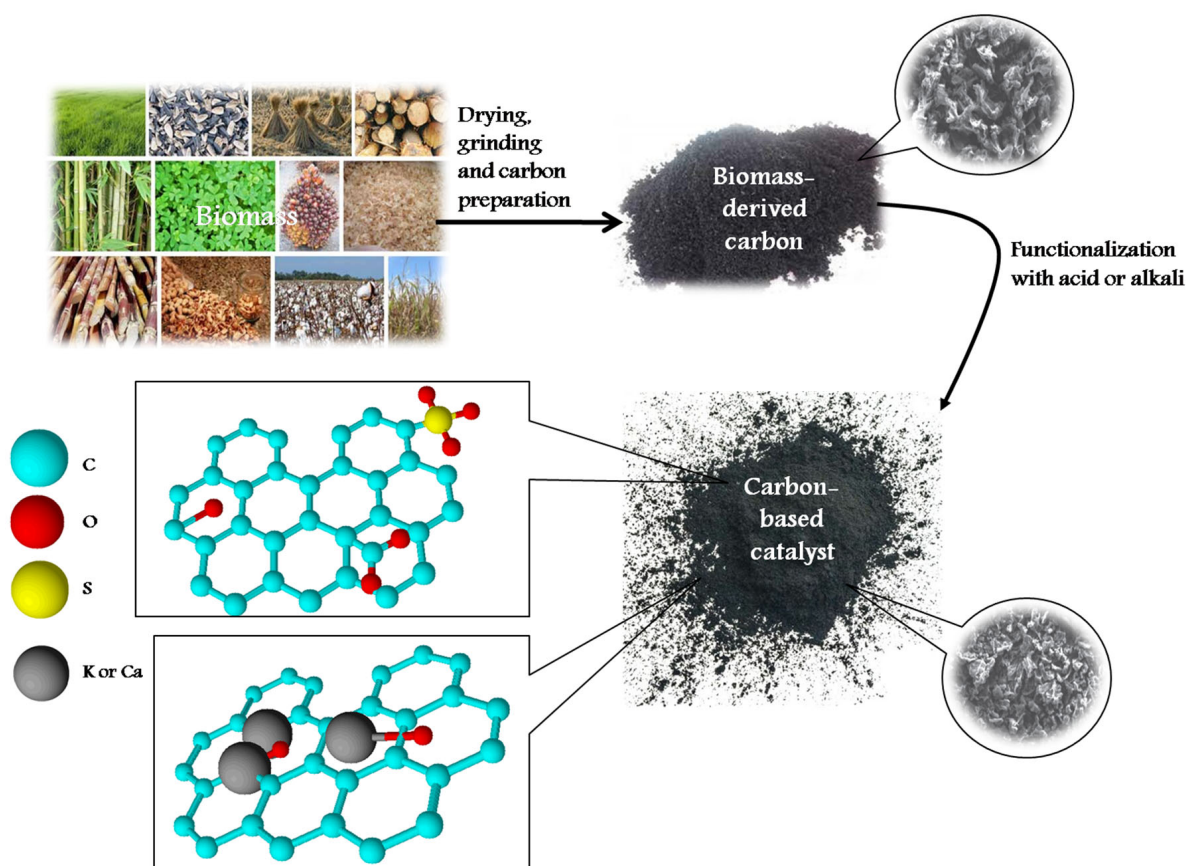


**Figure 2.** Biomass-derived carbons for the application in biodiesel production. Summarized from [23–46].

Table 1 presents the literature data on sulfonated carbon-based catalysts and their activity during the esterification/transesterification process.

**Table 1.** Sulfonated carbon-based catalysts for biodiesel production.

Biomass	Preparation Method	Oil Feedstock	Biodiesel Synthesis Conditions	Biodiesel Yield	SA *, m <sup>2</sup> /g	Reusability	Reference
<i>C. inophyllum</i> seeds	Carbonization for 5 h at 400 °C, followed by sulfonation by H <sub>2</sub> SO <sub>4</sub> (98 wt.%) at 150 °C.	<i>C. inophyllum</i> Oil	Oil/methanol ratio 1:30 mol, 0.3 g of catalyst, 150 °C, 2 h.	36.4	3.4	80% of initial activity at 2nd cycle	[23]
Starch	Pyrolysis for 5 h at 400 °C, followed by sulfonation by H <sub>2</sub> SO <sub>4</sub> (98 wt.%) at 150 °C.	<i>C. inophyllum</i> Oil	Oil/methanol ratio 1:30 mol, 7.5 wt.% of catalyst, 180 °C, 5 h.	81.0	0.9	80% of initial activity at 4th cycle	[24]
Glucose	Carbonization for 15 h at 400 °C, followed by sulfonation by H <sub>2</sub> SO <sub>4</sub> (98 wt.%) at 150 °C.	Oleic acid	Oleic acid/methanol ratio 1:50 mol, 5 wt.% of catalyst, 80 °C, 5 h.	95.0	4.1	93% of initial activity at 50th cycle	[19]
Starch	Pyrolysis for 3 h at 400 °C, followed by sulfonation by H <sub>2</sub> SO <sub>4</sub> (98 wt.%) at 150 °C.	Waste oil	Oil/methanol ratio 1:30 mol, 12 wt.% of catalyst, 80 °C, 15 h.	92.0	7.2	93% of initial activity at 50th cycle	[25]
Lignin	Pyrolysis for 1 h at 400 °C, followed by sulfonation by H <sub>2</sub> SO <sub>4</sub> (98 wt.%) at 150 °C.	Acidified soybean soapstock	Oil/methanol ratio 1:7 mol, 5 wt.% of catalyst, 70 °C, 5 h.	96.0	4.7	Over 90% of initial activity at 3rd cycle	[26]
Rice husk	Fast pyrolysis at 510 °C for 4 s, followed by sulfonation by H <sub>2</sub> SO <sub>4</sub> (98 wt.%) at 80 °C.	Waste oil	Oil/methanol ratio 1:30 mol, 10 wt.% of catalyst, 80 °C, 15 h.	90.0	4.0	-	[27]
Mesoporous starch	Carbonization for 5 h at 400 °C, followed by sulfonation by H <sub>2</sub> SO <sub>4</sub> (99 wt.%) at 80 °C.	Waste oil	Oil/methanol ratio 1:3 vol., 10 wt.% of catalyst, 80 °C, 18 h.	98.0	-	78% of initial activity at 4th cycle	[28]
Cotton stalk	Carbonization for 3 h at 450 °C, followed by sulfonation by H <sub>2</sub> SO <sub>4</sub> (98 wt.%) at 80 °C.	<i>Madhuca indica</i> oil	Oil/methanol ratio 1:18 mol, 5 wt.% of catalyst, 60 °C, 5 h.	89.2	92.0	90% of initial activity at 7th cycle	[29]
Waste banana peel	Treatment by 30 wt.% H <sub>3</sub> PO <sub>4</sub> , carbonization for 3 h at 600 °C, and then sulfonation by H <sub>2</sub> SO <sub>4</sub> (98 wt.%) at 80 °C.	Oleic acid	Oleic acid/methyl acetate ratio 1:50 mol, 12 wt.% of catalyst, 60 °C, 8 h.	52.3	-	82% of initial activity at 5th cycle	[30]
Waste cork	Pyrolysis for 2 h at 600 °C, followed by sulfonation by H <sub>2</sub> SO <sub>4</sub> (98 wt.%) at 80 °C.	Waste oil	Oil/methanol ratio 1:25 mol, 1.5 wt.% of catalyst, 65 °C, 6 h.	98.0	-	80% of initial activity at 5th cycle	[31]
Sugarcane bagasse	Treatment by H <sub>3</sub> PO <sub>4</sub> (1:1), calcination for 2 h at 400 °C, and then sulfonation by ClSO <sub>3</sub> H at 300 °C.	Palm fatty acid distillate (PFAD)	PFAD/methanol ratio 1:10 mol, 2 wt.% of catalyst, 60 °C, 1.5 h.	98.6	300.0	90% of initial activity at 6th cycle	[32]

\* SA—surface area.

Carbonization and pyrolysis of biomass with sulfonation result in a relatively low specific surface area of the catalyst. Meanwhile, pretreatment of biomass with phosphorous acid leads to a significant increase in the surface area three times that of non-pretreated ones [33]. Sulfonated biocarbon-based catalysts mainly show a FAME yield over 80 wt.%. It is observed that the catalyst activity slightly depends on the specific surface area of the catalysts, but the acid sites' density on the carbon surface plays an important role. However, a high surface area can be crucial for the reactions with large molecules (i.e., triglycerides). Thus, the catalyst surface area, acid site density, and carbon preparation method play important roles in the acid-catalyzed esterification/transesterification process.

However, one of the main problems for sulfonated carbon-based catalysts is the loss in activity after 5–7 cycles. Moreover, sulfonated catalysts tend to be deactivated at high temperatures because of the loss of sulfonic groups from the surface. Thus, future works should focus on the improvement of catalyst stability. Another challenge associated with oil transesterification in the presence of biomass-derived catalysts is the investigation of reaction kinetics and mechanisms.

## 2.2. Base-Functionalized Catalysts

Basic carbon-based catalysts are less used in the transesterification process in comparison to acidic ones. This is due to the high saponification activity of bases, especially

for HFFA oils [33]. Moreover, a critical disadvantage of a basic catalyst is its sensitivity to water [34]. Meanwhile, several studies on the application of base-functionalized carbon-based catalysts can be mentioned. Two directions in the preparation of base-functionalized carbon-based catalysts can be highlighted. The first one is calcination of biomass feedstock. As it is known, plant biomass contains a high amount of alkali and alkali-earth metals [4]. Calcination leads to a decrease in the concentration of H, O, and C atoms, producing alkali or alkali-metal oxides or hydroxides along with alumina or silicon oxides. The second method for base-functionalized catalyst preparation is preliminary treatment of raw biomass with solutions of KOH, potassium, or calcium salts (i.e., KF, Ca(Ac)<sub>2</sub>), followed by hydrothermal or thermal carbonization. This method results in a biochar containing metal oxides on the surface. The last ones catalyze the transesterification process and show high effectiveness. Table 2 presents the results of recent studies on transesterification of oils over a base-functionalized catalyst.

**Table 2.** Basic carbon-based catalysts for biodiesel production.

Biomass	Preparation Method	Oil Feedstock	Biodiesel Synthesis Conditions	Biodiesel Yield	SA *, m <sup>2</sup> /g	Reusability	Reference
Red banana peduncle	Calcination for 4 h at 700 °C.	<i>Ceiba pentandra</i> oil	Oil/methanol ratio 1:12 mol, 2.5 wt.% of catalyst, 65 °C, 2 h.	98.7	46.0	90% of initial activity at 3rd cycle	[35]
Banana peels	Calcination for 4 h at 700 °C.	<i>Bauhinia monandra</i> seed oil	Oil/methanol ratio 1:7.6 mol, 2.75 wt.% of catalyst, 65 °C, 70 min.	93.9	4.4	-	[36]
Coconut husk ash	Calcination for 1 h at 500 °C.	Jatropha oil	Oil/methanol ratio 1:12 mol, 7 wt.% of catalyst, 45 °C, 30 min.	90.0	-	-	[37]
Sugarcane bagasse	Treatment with 1M HCl, calcination for 4 h at 700 °C, treatment with 1 M NaOH, and carbonization at 300 °C for 1 h.	Waste oil	Oil/methanol ratio 1:2 vol., 10 wt.% of catalyst, 65 °C, 2 h.	99.0	-	-	[38]
Waste date seeds	Carbonization for 4 h at 450 °C, followed by impregnation by 1 M KOH and drying at room temperature for 48 h. HTC for 3 h at 250 °C, followed by impregnation by K <sub>2</sub> CO <sub>3</sub> and Cu(NO <sub>3</sub> ) <sub>2</sub> .	Waste oil	Oil/methanol ratio 1:10 mol, 3 wt.% of catalyst, 65 °C, 90 min.	93.0	260	-	[39]
Empty fruit bunch	Carbonization for 3 h at 600 °C, followed by impregnation by 1 M KOH.	Waste oil	Oil/methanol ratio 1:12 mol, 5 wt.% of catalyst, 70 °C, 2 h.	97.1	4056.2	80% of initial activity at 5th cycle	[40]
Coffee grounds	Carbonization for 3 h at 600 °C, followed by impregnation by 1 M KOH.	Waste oil	Oil/methanol ratio 1:9 mol, 5 wt.% of catalyst, 90 °C, 2 h.	91.6	-	80% of initial activity at 5th cycle	[41]
Raw coffee husks	Carbonization for 3 h at 700 °C, followed by impregnation by 1 M KOH.	Soybean oil	Oil/methanol ratio 1:10 mol, 10 wt.% of catalyst, 65 °C, 2 h.	74.0	-	90% of initial activity at 2nd cycle	[42]
Potato peel	Pyrolysis for 5 h at 500 °C, followed by calcination.	Waste oil	Oil/methanol ratio 1:9 mol, 3 wt.% of catalyst, 60 °C, 2 h.	97.5	-	90% of initial activity at 5th cycle	[43]
Hyacinth biomass	Carbonization for 8 h at 600 °C, followed by impregnation by K <sub>2</sub> CO <sub>3</sub> .	Palm oil	Oil/methanol ratio 1:12 mol, 15 wt.% of catalyst, 65 °C, 3 h.	97.6	-	-	[44]
Waste passion fruit peel	Calcination for 1 h at 500 °C	Palm oil	Oil/methanol ratio 1:15 mol, 7 wt.% of catalyst, room temperature, 30 min	95.4	-	78% of initial activity at 2nd cycle	[45]

\*SA—surface area.

The activity of base-functionalized catalysts is determined by both the base concentration and catalyst surface area. In this case, the surface area seems to be a significant factor, providing good triglyceride adsorption on the catalyst as well as the distribution and

availability of basic active sites. For this reason, the carbonization method (in particular, HTC) can be one of the most promising methods. Additionally, the use of additional alkali during the catalyst preparation process provides higher activity and biodiesel yield in comparison with catalysts obtained without impregnation.

Generally, base-functionalized carbon catalysts prepared through the calcination method are less stable and lose their activity after 3–5 consecutive cycles because of the leaching of alkali via water or methanol or because the interaction of alkali with free fatty acids. Meanwhile, catalysts prepared by the carbonization method, followed by activation by a base, maintain their effectiveness in terms of oil conversion of FAME yield for a minimum of five cycles. In spite of the lower stability, alkali catalysts allow transesterification to be performed at lower temperatures (even at room temperature) with a high biodiesel yield. This can be significant from an economical point of view.

In summary, basic biocarbon catalysts have proven to have a higher conversion of oil into biodiesel at a lower reaction temperature in comparison with sulfonated ones. However, the use of these composites in the transesterification of waste cooking oil is limited because of the high free fatty acid content in the oil.

### 3. Biomass-Derived Carbon-Based Catalysts for Biomass Conversion and Organic Synthesis

Sulfonated biomass-derived carbons have been effectively used for biomass conversion into valuable chemicals, such as furfural, 5-hydroxymethylfurfural, 5-ethoxymethylfurfural, and hexitols. The presence of  $-\text{SO}_3\text{H}$  groups on the carbon surface effectively catalyzes the hydrolysis and dehydration of polysaccharides of biomass (cellulose and hemicelluloses) (Figure 3) [15]. These catalysts are mainly produced by biomass pyrolysis with or without templates, followed by sulfonation by concentrated sulfuric acid. As for biodiesel synthesis, the resulting composites have the same structure and are characterized by high acidity. The summarized results are presented in Table 3.

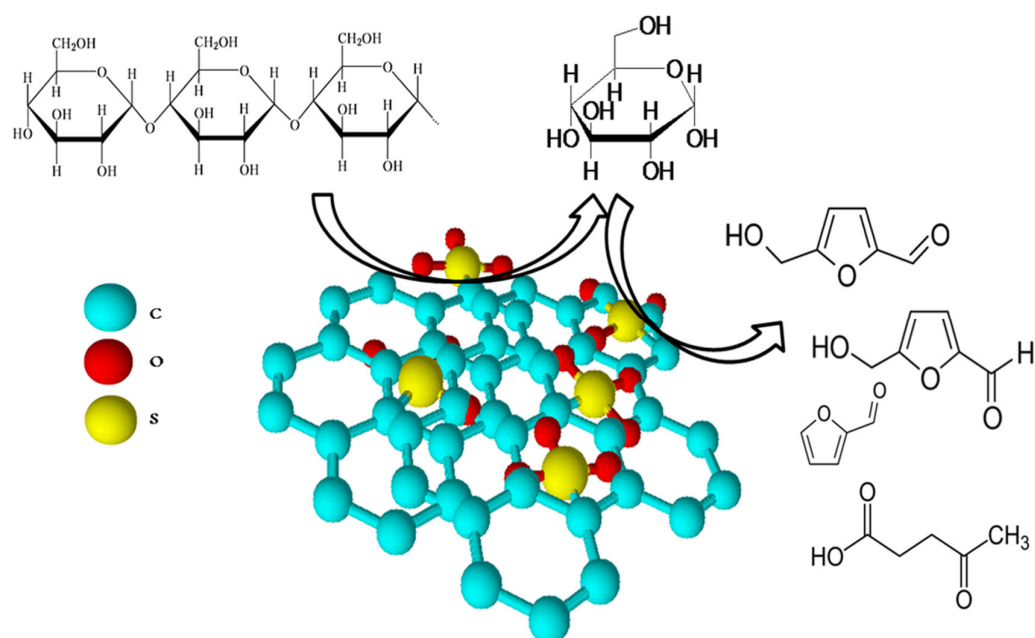


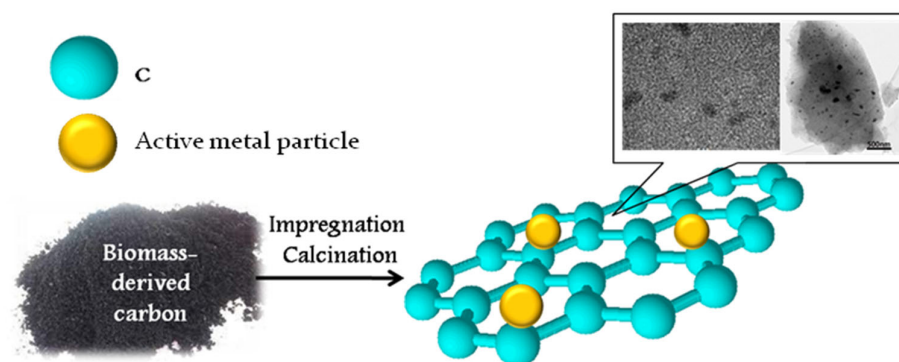
**Figure 3.** Application of acidic carbon-based catalysts for biomass conversion. Summarized from [46–55].

**Table 3.** Sulfonated carbon-based catalysts for biomass conversion.

Carbon Source	Feedstock	Reaction Conditions	Product	Product Yield, wt. %	Number of Cycles without Loss in Activity	Reference
Sucrose	Cellulose	110 °C, 4 h	Glucose	74.5	-	[46]
Microcrystalline cellulose	Eucalyptus flakes	120 °C, 3 h	Glucose	76.0	3	[47]
Glucose	Cellulose	110 °C, 4 h	Reducing sugars	72.7	5	[48]
Sucrose	Cellulose	120 °C, 4 h	Glucose	59.0	4	[49]
Cellulose	Cellulose	130 °C, 3 h	Reducing sugars	68.9	3	[50]
Glucose	Fructose	130 °C, 10 min	5-hydroxymethylfurfural	91.2	5	[51]
Cellulose	Fructose	80 °C, 10 min	5-hydroxymethylfurfural	83.0	5	[52]
Cornstalk	Cornstalk	170 °C, 30 min	Furfural	68.2	-	[53]
Waste <i>Camelia oleifera</i> shells	Fructose	100 °C, 24 h	5-ethoxymethylfurfural	25.0	4	[54]
Chestnut shell	Waste lignocellulose	180 °C, 15 min	Furfural	68.7	7	[55]

High catalytic activity of sulfonated carbons in biomass hydrolysis and dehydration reactions can be attributed to the high ability of SO<sub>3</sub>H-groups to adsorb carbohydrates, as well as their tolerance to hydration. Moreover, the catalyst effect in hydrolysis depends significantly on the water concentration and reaches a maximum when the water content is equal to the catalyst acidity [15,56]. In comparison with traditionally used catalysts containing Lewis and Brønsted acid sites (e.g., zeolites, Amberlyst, and Nafion), sulfonated carbons show higher effectiveness in biomass hydrolysis and dehydration and are considered promising for obtaining platform molecules from biomass.

Besides the functionalization of biocarbon with acid or basic sites, the production of carbon-based composites containing different metal nanoparticles is widely used. Carbon-supported catalysts have great potential in many organic reactions, such as hydrogenation, oxidation, alkylation, and dehydrohalogenation. Biomass-derived carbonaceous supports for metal-containing catalysts are effectively prepared through hydrothermal or dry carbonization, thus providing a high surface area for the resulting materials (200–1000 m<sup>2</sup>/g). The active metal-containing phase is traditionally formed by impregnation of the carbon supports with solutions of metal salts. Acetate and nitrates are widely used as metal precursors because of their easy decomposition by heating or calcination (Figure 4). A summary of the reactions using biomass-derived carbon-based catalysts is shown in Table 4.

**Figure 4.** Preparation of biochar-based metal-containing catalysts. Summarized from [57,58].

**Table 4.** Summary of biomass-derived carbon-based catalysts for organic reactions.

Carbon Source and Preparation Conditions	Active Phase	Substrate	Reaction Conditions	Product	Product Selectivity, wt.%	Number of Cycles without Loss in Activity	Reference
Hydrogenation							
Shrimp shell and pyrolysis at 600–800 °C for 2 h.	Core–shell Co@Co <sub>3</sub> O <sub>4</sub>	Nitroarenes	110 °C, 40 bar H <sub>2</sub> , 6 h	Amines	99.0	3	[57]
Bamboo shoots and HTS at 850 °C.	Core–shell Co@Co <sub>3</sub> O <sub>4</sub>	Nitroarenes	110 °C, 5 MPa H <sub>2</sub> , 5 h	Amines	>90.0	6	[58]
Bamboo shoots and HTS at 850 °C.	Pd	Alkynes	Room temperature, 1 atm H <sub>2</sub> , 7 h	Alkenes	95.0	-	[58]
Bamboo shoots and HTS at 850 °C.	Co/P	Nitroarenes	170 °C, formic acid as H-donor, 7 h	Amines	>97.0	-	[58]
Cornstalks and carbonization at 300 °C for 3 h.	Pt	Cinnamaldehyde	120 °C, 40 bar H <sub>2</sub> , 6 h	Hydrocinamyl alcohol	95.0	-	[59]
Starch and HTC at 500 °C.	Ru	Levulinic acid	150 °C, 5 MPa H <sub>2</sub> , 3 h	γ-valerolactone	99.0	5	[60]
Sucrose and HTS with poly(ionic liquid).	Au-Pd	Phenylacetylene	Room temperature, 1 atm H <sub>2</sub> , 7 h	Styrene	99.0	-	[61]
Other reactions							
Starch and gelation, followed by carbonization. Tannic acid and gel formation, followed by carbonization at 900 °C.	Fe <sub>3</sub> O <sub>4</sub>	Benzyl alcohol	130 °C, MW, 1 atm air	Benzaldehyde	74.0	5	[62]
Sugarcane bagasse and HTC at 600 °C.	Cu/Ni core-shell	Furfural		Methylfuran	48.0	4	[63]
Shrimp shell and pyrolysis at 600–800 °C for 2 h.	Ni/NiO, MgO	CH <sub>4</sub> + CO <sub>2</sub>	750 °C, 40 h	Synthesis gas	Methane conversion > 80%	5	[64]
Bamboo shoots and HTC at 850 °C.	Core–shell Co@Co <sub>3</sub> O <sub>4</sub>	Aryllhalides	130 °C, 30 bar H <sub>2</sub> , 24 h	Cycloalkenes	>90.0	4	[65]
Bamboo shoots and HTC at 850 °C.	Pd	Alkynes	Room temperature, 1 atm H <sub>2</sub> , 2.5 h	Vinylsilanes	96.0	-	[58]
Bamboo shoots and HTC at 850 °C.	Core–shell Co@Co <sub>3</sub> O <sub>4</sub>	Nitroarenes	110 °C, 5 MPa H <sub>2</sub> , 5 h	Structurally complex imines	81.0	-	[58]
Starch and carbonization at 600 °C.	Pd	Iodobenzene + methyl acrylate	130 °C, MW, 2 min, 0.1 g catalyst	Biaryles	95.0	2	[66]
Starch and carbonization at 600 °C.	Pd	Benzeneboronic acid + bromobenzene	130 °C, MW, 2 min, 0.1 g catalyst	Biaryles	99.0	3	[67]
Chitosan and carbonization at 750 °C.	Au	Phenylboronic acid	70 °C, 7 h, 0.01 g catalyst	biphenyl	86.0	-	[68]

Along with traditional carbon-based catalysts, biomass-derived ones exhibit high activity in different reactions. Moreover, the “green” nature of these systems makes them preferable for use in sustainable technologies. Carbon materials derived from biomass are considered to provide a high dispersion of metals deposited on their surface, as well as a narrow metal particle size distribution, leading to a higher reducibility of the active phase. Moreover, the presence of doped atoms (i.e., N and O) on the carbon surface increases the catalyst activity in comparison with traditional carbon-based catalysts. The higher surface area of the biocarbon-derived catalysts compared to those supported on inorganic



oxides (such as SiO<sub>2</sub> or Al<sub>2</sub>O<sub>3</sub>) also provides a good availability of active sites and higher hydrogen adsorption, resulting in their higher activity [15].

#### 4. Biomass-Derived Carbon-Based Catalysts for Electrocatalysis

Carbon-based materials are widely used as catalyst supports in electrocatalysis. Biomass-based carbon is a cheap and structured material that can be easily synthesized for large-scale applications. These supports can effectively replace existing electrocatalysts in the electrooxidation processes, hydrogen or oxygen evolution reactions (HER and ORR), and oxygen reduction reactions [15]. Electrocatalysts based on biomass-derived carbons have shown high activity and stable onset potential.

The structure of carbonaceous supports plays a great role in electrocatalysis. A higher activity has been shown by catalysts with a graphite- or grapheme-like structure. Biomass-based carbon catalysts as electrocatalysts are usually synthesized through pyrolysis or carbonization of biomass feedstock. The control over the synthesis process temperature, time of carbonization, and pyrolysis atmosphere are the key factors that allow the required structure of carbon-based catalysts to be obtained [15]. Moreover, the introduction of heteroatoms in the crystal lattice of carbon is a key factor for these electrocatalysts since it forms the active sites [69]. Doping usually serves as a charge transfer and modification of the electronic structure of carbon atoms (Figure 5). Among the doping heteroatoms, nitrogen, phosphorus, sulfur, and oxygen should be mentioned.

An overview of carbon-based electrocatalysts, their synthesis methods, structure, and onset potential is presented in Table 5.

**Table 5.** Summary of biomass-derived carbon-based electrocatalysts.

Catalyst	Carbon Source	Synthesis Conditions	Crystal Structure	Porosity	Onset Potential, V	Reaction	Catalyst Stability	Reference
Pd/N-C	Mildew-starting orange waste	Juice extraction, mixing with K <sub>2</sub> PdCl <sub>4</sub> , hydrothermal carbonization at 180 °C for 4 h, and pyrolysis in nitrogen atmosphere at 800 °C for 2 h.	Graphite-like structure with pyridinic and graphite N	Microporous, SA * = 26 m <sup>2</sup> /g	0.5	Methanol oxidation	90% in 50 cycles	[70]
N-C	N-rich yuba	Carbonization at 850 °C, followed by impregnation.	Graphite-like structure with pyridinic and pyrrolic N	Mesoporous, SA * = 740–1000 m <sup>2</sup> /g	0.97	Fuel cells	85% after 5000 s	[71]
Fe <sub>3</sub> C/C	Cellulose fiber	Impregnation with an iron salt, addition of dicyandiamide, carbonization, and etching. Impregnation with melanin, (MgOH) <sub>2</sub> CO <sub>3</sub> , and NaCl, carbonization at 900 °C, treatment with hemin, and calcination in nitrogen atmosphere.	Fe <sub>3</sub> C crystals over a graphite-like structure	-	0.98	Oxygen reduction	85% after 10,000 s	[72]
FeO <sub>x</sub> /N-C	Acorn shell	Impregnation with Fe(NO <sub>3</sub> ) <sub>3</sub> , calcinations at 950 °C for 5 h, and doping with nitrogen.	Graphite-like structure with pyridinic and pyrrolic N, Fe <sub>3</sub> O <sub>4</sub> , and Fe <sub>2</sub> O <sub>3</sub> coated with C	SA * = 819 m <sup>2</sup> /g	0.88 in ORR 0.72 in HRR	ORR and HRR	73% after 36,000 s	[73]
N-C	Wood char	Activation with alkali and doping with nitrogen.	Graphite-like structure with pyridinic and pyrrolic N	Microporous, SA * = 1924 m <sup>2</sup> /g	0.2	ORR	95% after 1200 min	[74]
Co/C	Cotton carbon fiber	Impregnation with CoCl <sub>2</sub> , ultrasonification, and carbonization at 900 °C for 3 h.	Graphite-like structure with amorphous carbon	Mesoporous, SA * = 358 m <sup>2</sup> /g	-	Lie-SeS <sub>2</sub> cells	70% after 45 cycles	[75]
Ru/N-C	Yeasts	Impregnation with RuCl <sub>3</sub> , calcinations at 950 °C for 5 h, and doping with nitrogen.	Graphite-like structure	-	0.2	HRR	85% after 60 h	[76]
Fe <sub>3</sub> O <sub>4</sub> /N-C	Yeasts	Impregnation with Fe(NO <sub>3</sub> ) <sub>3</sub> , calcinations at 950 °C for 5 h, and doping with nitrogen.	Graphite-like structure	-	0.3	ORR	85% after 60 h	[76]
Mo/C	Sugar beet, corn stover, pine, and miscanthus	Impregnation with Mo salt, pyrolysis at 600 °C for 6 h, and NaCl/NaF salt flux.	Graphite-like structure	-	0.3–0.5 V	HRR	-	[77]
N-C	Cocoon silk	Carbonization followed by activation by KOH.	Graphite-like structure with pyridinic and pyrrolic N	-	0.6	ORR	-	[78]
N-C	Cocoon silk	Pyrolysis followed by activation by ZnCl <sub>2</sub>	1D structure	-	0.85	ORR	95% after 12,000 s	[79]
N-C	Keratin	Precarbonization, activation with KOH, and treatment in ammonia at 1000 °C.	Grapheme-like 2D structure	-	0.8	ORR	92% after 300 s	[80]
N-C	Coconut shell	Carbonization followed by activation by H <sub>3</sub> PO <sub>4</sub> .	Graphite-like structure	Mesoporous, SA * = 1260 m <sup>2</sup> /g	-	ORR	90% after 12 h	[81]
N-C	Ophiopogon japonicus	Hydrothermal carbonization at 180 °C.	Carbon nanodot/nanosheet aggregates	-	0.88	ORR	-	[82]
N-C	Basswood	Pyrolysis at 600 °C and activation in ammonia atmosphere.	Graphite-like structure	SA * = 1438 m <sup>2</sup> /g	0.98	ORR	95% after 20 h	[83]
N-C	Pinecone	Precarbonization at 800 °C and activation in ammonia.	Graphite-like structure	-	0.95	ORR	-	[84]
N-C	Spent coffee grounds	Pyrolysis followed by activation by KOH.	Graphite-like structure	SA * = 1018 m <sup>2</sup> /g	0.94	ORR	95% after 10,000 s	[85]
N-C	Banana peels	Carbonization followed by activation by KOH, and treatment with ammonia	Graphite-like structure	SA * = 1756 m <sup>2</sup> /g	0.98	ORR	95% after 10,000 s	[86]

\* SA—surface area.

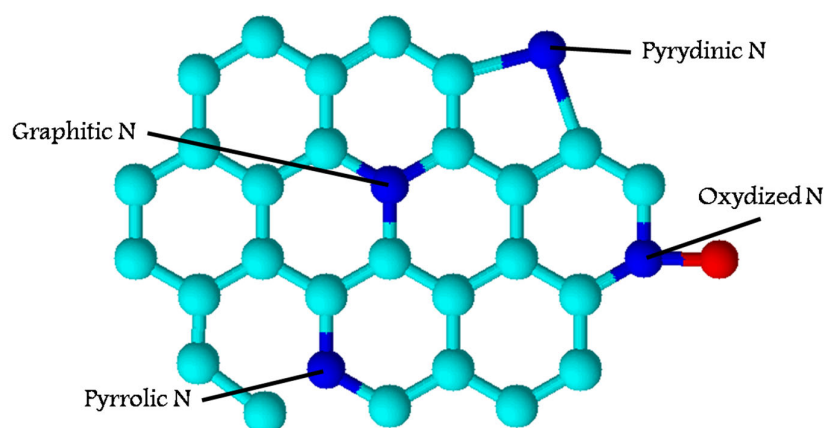


**Figure 5.** Overall structure of N-doped carbon-based electrocatalyst. Summarized from [69,70,73,77–85].

For electrocatalysts, the distribution of metal-containing particles and heteroatoms, the crystal structure of carbonaceous support, and its porosity play a great role. It has been shown that the presence of heteroatoms exhibits a higher catalytic activity than that of non-doped carbons, as well as a higher potential stability. The hierarchical porous structure can also improve the activity of these electrocatalysts in most reactions because of the facilitation of the diffusion of reactants and products [69,87]. A high surface area of the electrodes obtained from biocarbons is crucial for the energy storage and ion/electron transport. Thus, biomass-derived carbonaceous materials can be effectively applied as supercapacitors. Biomass-derived carbon electrodes can be considered a promising alternative to traditional electrodes [87].

## 5. Conclusions and Future Prospective

The key requirements that catalysts should meet are high activity and selectivity toward the target products, stability in the reaction medium, mechanical effects, and temperature. In terms of structure, heterogeneous catalysts should have a uniform distribution of the active phase, thus avoiding its aggregation; high porosity to allow reagent molecules to easily reach the active sites; and a proper structure of the active sites to catalyze the target reactions. Therefore, the catalyst design is of great interest.

Carbon-based catalysts have attracted much attention in recent years. Their low cost, simple preparation methods, and “green” nature make carbon materials a promising support for catalysts. Biomass can be successfully used for the preparation of carbon-based catalysts through different methods, mainly based on thermochemical decomposition. Different types of biomasses, e.g., starch, lignin, cellulose, chitosan, wood, agricultural or food waste, and marine waste, can be promising carbon feedstock. Expanding biomass sources, development of new methods for direct catalyst synthesis, expanding the choice of synthesis conditions, and development of “green” preparation methods are the main directions for future research for biomass-derived catalyst synthesis. Moreover, wider applications of biomass-derived catalysts, including electrocatalysis, fine and organic synthesis, and flow processes, should be developed to provide sustainable and environmentally friendly processes.

**Author Contributions:** Conceptualization, A.A.S. and M.G.S.; data collection, Y.V.L. and Y.Y.K.; writing—original draft preparation, A.A.S. and V.G.M.; writing—review and editing, M.E.M.; project administration, A.A.S. All authors have read and agreed to the published version of the manuscript.

**Funding:** The financial support for this work was provided by the Russian Science Foundation (grant 22-79-10096).

**Data Availability Statement:** Not applicable.

**Conflicts of Interest:** The authors declare no conflict of interest.

## References

1. Elliott, D.C.; Hart, T.R. Catalytic hydroprocessing of chemical models for bio-oil. *Energy Fuels* **2008**, *23*, 631–637. [\[CrossRef\]](#)
2. Sharma, S.; Pollet, B.G. Support materials for PEMFC and DMFC electrocatalysts—A review. *J. Power Sources* **2012**, *208*, 96–119. [\[CrossRef\]](#)
3. Lam, E.; Luong, J.H.T. Carbon Materials as Catalyst Supports and Catalysts in the Transformation of Biomass to Fuels and Chemicals. *ACS Catal.* **2014**, *4*, 3393–3410. [\[CrossRef\]](#)
4. Maroa, S.; Inambao, F. A review of sustainable biodiesel production using biomass-derived heterogeneous catalysts. *Eng. Life Sci.* **2021**, *21*, 790–824. [\[CrossRef\]](#) [\[PubMed\]](#)
5. Alrobaian, A.; Rajasekar, V.; Alagumalai, A. Critical insight into biowaste-derived biocatalyst for biodiesel production. *Environ. Prog. Sustain. Energy* **2020**, *39*, e13391. [\[CrossRef\]](#)
6. Smith, S.M.; Oopathum, C.; Weeramongkhonlert, V.; Smith, C.B. Transesterification of soybean oil using bovine bone waste as new catalyst. *Bioresour. Technol.* **2013**, *143*, 686–690. [\[CrossRef\]](#)
7. Roschat, W.; Kacha, M.; Yoosuk, B.; Sudyoasuk, T. Biodiesel production based on heterogeneous process catalyzed by solid waste coral fragment. *Fuel* **2012**, *98*, 194–202. [\[CrossRef\]](#)
8. Pang, S. Advances in thermochemical conversion of woody biomass to energy, fuels and chemicals. *Biotechnol. Adv.* **2019**, *37*, 589–597. [\[CrossRef\]](#)
9. Yaashikaa, P.R.; Kumar, P.S.; Varjani, S.; Saravanan, A. A critical review on the biochar production techniques, characterization, stability and applications for circular bioeconomy. *Biotechnol. Rep.* **2020**, *28*, e00570. [\[CrossRef\]](#)
10. Cantrell, K.B.; Hunt, P.G.; Uchimiya, M.; Novak, J.M.; Ro, K.S. Impact of pyrolysis temperature and manure source on physico-chemical characteristics of biochar. *Bioresour. Technol.* **2012**, *107*, 419–428. [\[CrossRef\]](#)
11. Nunoura, T.; Wade, S.R.; Bourke, J.P.; Antal, M.J. Studies of the flash carbonization process. 1. Propagation of the flaming pyrolysis reaction and performance of a catalytic afterburner. *Ind. Eng. Chem. Res.* **2006**, *45*, 585–599. [\[CrossRef\]](#)
12. Funke, A.; Ziegler, F. Hydrothermal carbonization of biomass: A summary and discussion of chemical mechanisms for process engineering. *Biofuels Bioprod. Biorefin.* **2010**, *4*, 160–177. [\[CrossRef\]](#)
13. Titirici, M.-M.; Thomas, A.; Antonietti, M. Back in the black: Hydrothermal carbonization of plant material as an efficient chemical process to treat the CO<sub>2</sub> problem? *New J. Chem.* **2007**, *31*, 787–789. [\[CrossRef\]](#)
14. Titirici, M.-M.; White, R.J.; Brun, N.; Budarin, V.L.; Su, D.S.; del Monte, F.; Clark, J.H.; MacLachlan, M.J. Sustainable carbon materials. *Chem. Soc. Rev.* **2015**, *44*, 250–290. [\[CrossRef\]](#)
15. De, S.; Balu, A.M.; van der Waal, J.C.; Lique, R. Biomass-Derived Porous Carbon Materials: Synthesis and Catalytic Applications. *ChemCatChem* **2015**, *7*, 1608–1629. [\[CrossRef\]](#)
16. Klinghoffer, N.B.; Castaldi, M.J.; Nzihou, A. Influence of char composition and inorganics on catalytic activity of char from biomass gasification. *Fuel* **2015**, *157*, 37–47. [\[CrossRef\]](#)
17. Bergman, P.C.A.; Boersma, A.R.; Zwart, R.W.R.; Kiel, J.H.A. *Torrefaction for Biomass Co-Firing in Existing Coal-Fired Power Stations*; Report No. ECNCO5013 Energy Research Centre of The Netherlands (ECN); Energy Research Centre of The Netherlands: Petten, The Netherlands, 2005; p. 71.
18. Shokrolahi, A.; Zali, A.; Keshavarz, M.H. Wet carbon-based solid acid/NaNO<sub>3</sub> as a mild and efficient reagent for nitration of aromatic compound under solvent free conditions. *Chin. Chem. Lett.* **2007**, *18*, 1064–1066. [\[CrossRef\]](#)
19. Zong, M.H.; Duan, Z.Q.; Lou, W.Y.; Smith, T.J.; Wu, H. Preparation of a sugar catalyst and its use for highly efficient production of biodiesel. *Green Chem.* **2007**, *5*, 434–437. [\[CrossRef\]](#)
20. Lokman, I.M.; Rashid, U.; Yunus, R.; Taufiq-Yap, Y.H. Carbohydrate-derived Solid Acid Catalysts for Biodiesel Production from Low-Cost Feedstocks: A Review. *Catal. Rev. Sci. Eng.* **2014**, *56*, 187–219. [\[CrossRef\]](#)
21. Hara, M.; Yoshida, T.; Takagaki, A.; Takata, T.; Kondo, J.N.; Domen, K.; Hayashi, S. A carbon material as a strong protonic acid. *Angew. Chem. Int. Ed.* **2004**, *43*, 2955–2958. [\[CrossRef\]](#)
22. Shu, Q.; Zhang, Q.; Xu, G.; Nawaz, Z.; Wang, D.; Wang, J. Synthesis of biodiesel from cottonseed oil and methanol using a carbon-based solid acid catalyst. *Fuel Process. Technol.* **2009**, *90*, 1002–1008. [\[CrossRef\]](#)
23. Dawodu, F.A.; Ayodele, O.O.; Xina, J.; Zhanga, S. Application of solid acid catalyst derived from low value biomass for a cheaper biodiesel production. *J. Chem. Technol. Biotechnol.* **2014**, *89*, 1898–1909. [\[CrossRef\]](#)
24. Ayodele, O.O.; Dawodu, F.A. Conversion of Calophyllum inophyllum Oil with a High Free Fatty Acid Content to Biodiesel using a Starch-Derived Catalyst. *Energy Technol.* **2014**, *2*, 912–920. [\[CrossRef\]](#)
25. Lou, W.Y.; Zong, M.H.; Duan, Z.Q. Efficient production of biodiesel from high free fatty acid-containing waste oils using various carbohydrate-derived solid acid catalysts. *Bioresour. Technol.* **2008**, *99*, 8752–8758. [\[CrossRef\]](#)
26. Guo, F.; Xiu, Z.L.; Liang, Z.X. Synthesis of biodiesel from acidified soybean soapstock using a lignin-derived carbonaceous catalyst. *Appl. Energy* **2012**, *98*, 47–52. [\[CrossRef\]](#)
27. Li, M.; Zheng, Y.; Chen, Y.; Zhu, X. Biodiesel production from waste cooking oil using a heterogeneous catalyst from pyrolyzed rice husk. *Bioresour. Technol.* **2014**, *154*, 345–348. [\[CrossRef\]](#)
28. Luque, R.; Clark, J.H. Biodiesel-Like Biofuels from Simultaneous Transesterification/Esterification of Waste Oils with a Biomass-Derived Solid Acid Catalyst. *ChemCatChem* **2011**, *3*, 594–597. [\[CrossRef\]](#)
29. Choksi, H.; Pandian, S.; Gandhi, Y.H.; Deepalakshmi, S. Studies on production of biodiesel from Madhuca indica oil using a catalyst derived from cotton stalk. *Energy Sources Part A Recovery Util. Environ. Eff.* **2019**, *43*, 3424–3433. [\[CrossRef\]](#)

30. Wong, W.-Y.; Lim, S.; Pang, Y.-L.; Chen, W.-H.; Lam, M.-K.; Tan, I.-S. Synthesis of glycerol-free fatty acid methyl ester using transesterification reaction based on solid acid carbon catalyst derived from low-cost biomass wastes. *Int. J. Energy Res.* **2020**, *46*, 147–162. [[CrossRef](#)]
31. Bhatia, S.K.; Gurav, R.; Choi, T.-R.; Kim, H.J.; Yang, S.-Y.; Song, H.-S.; Park, J.Y.; Park, Y.-L.; Han, Y.-H.; Choi, Y.-K. Conversion of waste cooking oil into biodiesel using heterogeneous catalyst derived from cork biochar. *Bioresour. Technol.* **2020**, *302*, 122872. [[CrossRef](#)]
32. Akinfalabi, S.-I.; Rashid, U.; Ngamcharussrivichai, C.; Nehdi, I.A. Synthesis of reusable biobased nano-catalyst from waste sugarcane bagasse for biodiesel production. *Environ. Technol. Innov.* **2020**, *18*, 100788–100801. [[CrossRef](#)]
33. Meher, L.; Churamani, C.; Arif, M.; Ahmed, Z.; Naik, S. *Jatropha curcas* as a renewable source for bio-fuels—A review. *Renew. Sustain. Energy Rev.* **2013**, *26*, 397–407. [[CrossRef](#)]
34. Leung, D.; Guo, Y. Transesterification of neat and used frying oil: Optimization for biodiesel production. *Fuel Process. Technol.* **2006**, *87*, 883–890. [[CrossRef](#)]
35. Balajii, M.; Niju, S. A novel biobased heterogeneous catalyst derived from *Musa acuminata* peduncle for biodiesel production—Process optimization using central composite design. *Energy Convers. Manag.* **2019**, *189*, 118–131. [[CrossRef](#)]
36. Betiku, E.; Akintunde, A.M.; Ojumu, T.V. Banana peels as a biobase catalyst for fatty acid methyl esters production using Napoleon's plume (*Bauhinia monandra*) seed oil: A process parameters optimization study. *Energy* **2016**, *103*, 797–806. [[CrossRef](#)]
37. Vadery, V.; Narayanan, B.N.; Ramakrishnan, R.M.; Cherikkallinmel, S.K.; Sugunan, S.; Narayanan, D.P.; Sasidharan, S. Room temperature production of *jatropha* biodiesel over coconut husk ash. *Energy* **2014**, *70*, 588–594. [[CrossRef](#)]
38. Niju, S.; Kanna, S.K.A.; Ramalingam, V.; Kumar, M.S.; Balajii, M. Sugarcane bagasse derived biochar—A potential heterogeneous catalyst for transesterification process. *Energy Sources Part A Recovery Util. Environ. Eff.* **2019**, *20*, 1–12. [[CrossRef](#)]
39. Inayat, A.; Jamil, F.; Raza, F.; Khurram, S.; Ghenai, C.; Al-Muhateb, A.H. Upgradation of waste cooking oil to biodiesel in the presence of green catalyst derived from date seeds. *Biofuels* **2021**, *12*, 1245–1250. [[CrossRef](#)]
40. Abdullah, R.F.; Rashid, U.; Hazmi, B.; Ibrahim, M.L.; Tsubota, T.; Alharthi, F.A. Potential heterogeneous nano-catalyst via integrating hydrothermal carbonization for biodiesel production using waste cooking oil. *Chemosphere* **2022**, *286*, 131913. [[CrossRef](#)]
41. Atelge, M. Production of biodiesel and hydrogen by using a double-function heterogeneous catalyst derived from spent coffee grounds and its thermodynamic analysis. *Renew. Energy* **2022**, *198*, 1–15. [[CrossRef](#)]
42. Fernández, J.V.; Faria, D.N.; Santoro, M.C.; Mantovaneli, R.; Cipriano, D.F.; Brito, G.M.; Carneiro, M.T.W.; Schettino, M.A.; Gonzalez, J.L.; Freitas, J.C. Use of Unmodified Coffee Husk Biochar and Ashes as Heterogeneous Catalysts in Biodiesel Synthesis. *BioEnergy Res.* **2022**. [[CrossRef](#)]
43. Daimary, N.; Eldiehy, K.S.; Boruah, P.; Deka, D.; Bora, U.; Kakati, B.K. Potato peels as a sustainable source for biochar, bio-oil and a green heterogeneous catalyst for biodiesel production. *J. Environ. Chem. Eng.* **2022**, *10*, 107108. [[CrossRef](#)]
44. Yani, F.; Ulhaqi, R.; Pratiwi, W.; Pontas, K.; Husin, H. Utilization of water hyacinth-based biomass as a potential heterogeneous catalyst for biodiesel production. *J. Phys. Conf. Ser.* **2019**, *1402*, 055005. [[CrossRef](#)]
45. Tarigan, J.B.; Singh, K.; Sinuraya, J.S.; Supeno, M.; Sembiring, H.; Tarigan, K.; Rambe, S.M.; Karo-Karo, J.A.; Sitepu, E.K. Waste Passion Fruit Peel as a Heterogeneous Catalyst for Room-Temperature Biodiesel Production. *ACS Omega* **2022**, *7*, 7885–7892. [[CrossRef](#)]
46. Pang, J.; Wang, A.; Zheng, M.; Zhang, T. Hydrolysis of cellulose into glucose over carbons sulfonated at elevated temperatures. *Chem. Commun.* **2010**, *46*, 6935–6937. [[CrossRef](#)]
47. Sukanuma, S.; Nakajima, K.; Kitano, M.; Yamaguchi, D.; Kato, H.; Hayashi, S.; Hara, M. Hydrolysis of Cellulose by Amorphous Carbon Bearing SO<sub>3</sub>H, COOH, and OH Groups. *J. Am. Chem. Soc.* **2008**, *130*, 12787–12793. [[CrossRef](#)]
48. Guo, H.; Qi, X.; Li, L.; Smith, R.L., Jr. Hydrolysis of cellulose over functionalized glucose-derived carbon catalyst in ionic liquid. *Bioresour. Technol.* **2012**, *116*, 355–359. [[CrossRef](#)]
49. Liu, M.; Jia, S.; Gong, Y.; Song, C.; Guo, X. Effective hydrolysis of cellulose into glucose over sulfonated sugar-derived carbon in an ionic liquid. *Ind. Eng. Chem. Res.* **2013**, *52*, 8167–8173. [[CrossRef](#)]
50. Guo, H.; Lian, Y.; Yan, L.; Qi, X.; Smith, R.L., Jr. Cellulose-derived superparamagnetic carbonaceous solid acid catalyst. *Green Chem.* **2013**, *15*, 2167–2174. [[CrossRef](#)]
51. Wang, J.J.; Xu, W.J.; Ren, J.W.; Liu, X.H.; Lu, G.Z.; Wang, Y.Q. Efficient catalytic conversion of fructose into hydroxymethylfurfural by a novel carbon-based solid acid. *Green Chem.* **2011**, *13*, 2678–2681. [[CrossRef](#)]
52. Qi, X.H.; Guo, H.X.; Li, L.Y.; Smith, R.L., Jr. Acid-Catalyzed Dehydration of Fructose into 5-Hydroxymethylfurfural by Cellulose-Derived Amorphous Carbon. *ChemSusChem* **2012**, *5*, 2215–2220. [[CrossRef](#)]
53. Ji, L.; Tang, Z.; Yang, D.; Ma, C.; He, Y.-C. Improved one-pot synthesis of furfural from corn stalk with heterogeneous catalysis using corn stalk as biobased carrier in deep eutectic solvent–water system. *Bioresour. Technol.* **2021**, *340*, 125691–125699. [[CrossRef](#)]
54. Wen, Y.; Yu, Z.; Li, K.; Guo, H.; Dai, Y.; Yan, L. Fabrication of biobased heterogeneous solid Brønsted acid catalysts and their application on the synthesis of liquid biofuel 5-ethoxymethylfurfural from fructose. *Green Energy Environ.* **2018**, *3*, 384–391. [[CrossRef](#)]
55. Liang, J.; Zha, J.; Zhao, N.; Tang, Z.; He, Y.; Ma, C. Valorization of Waste Lignocellulose to Furfural by Sulfonated Biobased Heterogeneous Catalyst Using Ultrasonic-Treated Chestnut Shell Waste as Carrier. *Processes* **2021**, *9*, 2269. [[CrossRef](#)]

56. Kang, S.; Ye, J.; Chang, J. Recent Advances in Carbon-Based Sulfonated Catalyst: Preparation and Application. *Int. Rev. Chem. Eng.* **2013**, *5*, 133–144.
57. Sahoo, B.; Formenti, D.; Topf, C.; Bachmann, S.; Scalone, M.; Junge, K.; Beller, M. Sustainable Biomass-Derived Catalysts for Selective Hydrogenation of Nitroarenes. *ChemSusChem* **2017**, *10*, 3035–3039. [[CrossRef](#)]
58. Song, T.; Yang, Y. Metal Nanoparticles Supported on Biomass-Derived Hierarchical Porous Heteroatom-Doped Carbon from Bamboo Shoots Design, Synthesis and Applications. *Chem. Rec.* **2018**, *19*, 1283–1301. [[CrossRef](#)]
59. Zhang, F.; Li, G.-D.; Chen, J.-S. Preparation and gas storage of high surface area microporous carbon derived from biomass source cornstalks. *J. Colloid Interface Sci.* **2008**, *327*, 108–114. [[CrossRef](#)]
60. Luque, R.; Clark, J.H. Water-tolerant Ru-Starbon (R) materials for the hydrogenation of organic acids in aqueous ethanol. *Catal. Commun.* **2010**, *11*, 928–931. [[CrossRef](#)]
61. Zhang, P.; Yuan, J.; Fellingner, T.-P.; Antonietti, M.; Li, H.; Wang, Y. Improving hydrothermal carbonization by using poly(ionic liquid)s. *Angew. Chem. Int. Ed.* **2013**, *52*, 6028–6032. [[CrossRef](#)]
62. Ojeda, M.; Balu, A.M.; Romero, A.A.; Esquinazi, P.; Ruokolainen, J.; Sixta, H.; Luque, R. MAGBONS: Novel Magnetically Separable Carbonaceous Nanohybrids from Porous Polysaccharides. *ChemCatChem* **2014**, *6*, 2847–2853. [[CrossRef](#)]
63. Varila, T.; Makela, E.; Kupila, R.; Romar, H.; Hu, T.; Karinen, R.; Puurunen, R.L.; Lassi, U. Conversion of furfural to 2-methylfuran over CuNi catalysts supported on biobased carbon foams. *Catal. Today* **2021**, *367*, 16–27. [[CrossRef](#)]
64. Liang, Y.; Han, J.; Wang, H.; Zhao, B.; Qin, L.; Wang, Y. Synthesis of Ni-Mg@HC catalyst derived from sugarcane bagasse and its application for producing syngas via CO<sub>2</sub> dry reforming. *Energy Sources Part A Recovery Util. Environ. Eff.* **2019**, *18*, 1–14. [[CrossRef](#)]
65. Sahoo, B.; Surkus, A.-E.; Pohl, M.-M.; Radnik, J.; Schneider, M.; Bachmann, S.; Scalone, M.; Junge, K.; Beller, M. A Biomass-Derived Non-Noble Cobalt Catalyst for Selective Hydrodehalogenation of Alkyl and (Hetero)Aryl Halides. *Angew. Chem.* **2017**, *129*, 11394–11399. [[CrossRef](#)]
66. Gronnow, M.J.; Luque, R.; Macquarrie, D.J.; Clark, H. A novel highly active biomaterial supported palladium catalyst. *Green Chem.* **2005**, *7*, 552–557. [[CrossRef](#)]
67. Budarin, V.L.; Clark, J.H.; Luque, R.; Macquarrie, D.J.; White, R.J. Versatile mesoporous carbonaceous materials for acid catalysis. *Green Chem.* **2008**, *10*, 382–387. [[CrossRef](#)]
68. Sk, M.P.; Jana, C.K.; Chattopadhyay, A. A gold-carbon nanoparticle composite as an efficient catalyst for homocoupling reaction. *Chem. Commun.* **2013**, *49*, 8235–8237.
69. Zhang, Z.; Yang, S.; Li, H.; Zan, Y.; Li, X.; Zhu, Y.; Dou, M.; Wang, F. Sustainable Carbonaceous Materials Derived from Biomass as Metal-Free Electrocatalysts. *Adv. Mater.* **2019**, *31*, 1805718. [[CrossRef](#)]
70. Da, Z.; Niu, X.; Li, X.; Zhang, W.; He, Y.; Pan, J.; Qui, F.; Yan, Y. From mildewy orange waste to natural reductant and catalyst support: Active palladium/biomass-derived carbonaceous hybrids for promoted methanol electro-oxidation. *ChemElectroChem* **2017**, *4*, 1372–1377. [[CrossRef](#)]
71. Zhang, J.J.; Sun, Y.; Guo, L.K.; Sun, X.N.; Huang, N.B. Ball-Milling Effect on Biomass-Derived Nanocarbon Catalysts for the Oxygen Reduction Reaction. *ChemistrySelect* **2021**, *6*, 6019–6028. [[CrossRef](#)]
72. Wei, J.; Liang, Y.; Hu, Y.; Kong, B.; Simon, G.P.; Zhang, J.; Jiang, S.P.; Wang, H. A Versatile Iron-Tannin-Framework Ink Coating Strategy to Fabricate Biomass-Derived Iron Carbide/Fe-N-Carbon Catalysts for Efficient Oxygen Reduction. *Agnew. Chem. Int. Ed.* **2016**, *55*, 1355–1359. [[CrossRef](#)]
73. Lu, Z.; Chen, J.; Wang, W.L.; Li, W.; Sun, M.; Wang, Y.; Wang, X.; Ye, J.; Rao, H. Electrocatalytic, Kinetic, and Mechanism Insights into the Oxygen-Reduction Catalyzed Based on the Biomass-Derived FeO<sub>x</sub>@N-Doped Porous Carbon Composites. *Small* **2021**, *17*, 2007326. [[CrossRef](#)]
74. Kaare, K.; Yu, E.; Käämbre, T.; Volperts, A.; Dobeles, G.; Zhurinsh, A.; Niaura, G.; Tamasauskaitė-Tamasiunaite, L.; Norkus, E.; Kruusenberg, I. Biomass-derived Graphene-like Catalyst Material for Oxygen Reduction Reaction. *ChemNanoMat* **2021**, *7*, 307–313. [[CrossRef](#)]
75. Zhang, Y.; Wang, B.; Jing, P.; Guo, Y.; Zhang, Y.; Wei, Y.; Wang, Q.; Zhang, Y.; Wu, H. Bioderived carbon fiber conductive networks with inlaid electrocatalysts as an ultralight freestanding interlayer for working Li-FeS<sub>2</sub> pouch cells. *Carbon* **2022**, *189*, 10–20. [[CrossRef](#)]
76. Tiwari, J.N.; Dang, N.K.; Sultan, S.; Thangavel, P.; Jeong, H.Y.; Kim, K.S. Multi-heteroatom-doped carbon from waste-yeast biomass for sustained water splitting. *Nature Sust.* **2020**, *3*, 556–563. [[CrossRef](#)]
77. Harris, D.; Budhi, S.; She, Y.; Henry, J.; Leonard, B.M. Biomass derived metal carbide catalysts formed using a salt flux synthesis. *Mater. Res. Express* **2019**, *6*, 115519. [[CrossRef](#)]
78. Wang, Y.; Lei, Y.; Wang, H. Astridia velutina-like S, N-codoped hierarchical porous carbon from silk cocoon for superior oxygen reduction reaction. *RSC Adv.* **2016**, *6*, 73560–73565. [[CrossRef](#)]
79. Fu, P.; Zhou, L.; Sun, L.; Huang, B.; Yuan, Y. Nitrogen-doped porous activated carbon derived from cocoon silk as a highly efficient metal-free electrocatalyst for the oxygen reduction reaction. *RSC Adv.* **2017**, *7*, 13383–13389. [[CrossRef](#)]
80. Zhang, J.; Zhou, H.; Liu, X.; Zhang, J.; Peng, T.; Yang, J.; Huang, Y.; Mu, S. Keratin-derived S/N co-doped graphene-like nanobubble and nanosheet hybrids for highly efficient oxygen reduction. *J. Mater. Chem. A* **2016**, *4*, 15870–15879. [[CrossRef](#)]

81. Borghei, M.; Laocharoen, N.; Kibena-Pöldsepp, E.; Johansson, L.S.; Campbell, J.; Kauppinen, E.; Tammeveski, K.; Rojas, O.J. Porous N,P-doped carbon from coconut shells with high electrocatalytic activity for oxygen reduction. *Appl. Catal. B* **2017**, *204*, 394–402. [[CrossRef](#)]
82. Oh, J.; Park, S.; Jang, D.; Shin, Y.; Lim, D.; Park, S. Metal-free N-doped carbon blacks as excellent electrocatalysts for oxygen reduction reactions. *Carbon* **2019**, *145*, 481–487. [[CrossRef](#)]
83. Tang, Z.; Pei, Z.; Wang, Z.; Li, H.; Zeng, J.; Ruan, Z.; Huang, Y.; Zhu, M.; Xue, Q.; Yu, J.; et al. Highly anisotropic, multichannel wood carbon with optimized heteroatom doping for supercapacitor and oxygen reduction reaction. *Carbon* **2018**, *130*, 532–538. [[CrossRef](#)]
84. Lei, X.; Wang, M.; Lai, Y.; Hu, L.; Wang, H.; Fang, Z.; Li, J.; Fang, J. Nitrogen-doped micropore-dominant carbon derived from waste pine cone as a promising metal-free electrocatalyst for aqueous zinc/air batteries. *J. Power Sources* **2017**, *365*, 76–82. [[CrossRef](#)]
85. Srinu, A.; Peera, S.G.; Parthiban, V.; Bhuvaneshwari, B.; Sahu, A.K. Heteroatom Engineering and Co-Doping of N and P to Porous Carbon Derived from Spent Coffee Grounds as an Efficient Electrocatalyst for Oxygen Reduction Reactions in Alkaline Medium. *ChemistrySelect* **2018**, *3*, 690–702. [[CrossRef](#)]
86. Zhang, J.; Zhang, C.; Zhao, Y.; Amiin, I.S.; Zhou, H.; Liu, X.; Tang, Y.; Mu, S. Three dimensional few-layer porous carbon nanosheets towards oxygen reduction. *Appl. Catal. B* **2017**, *211*, 148–156. [[CrossRef](#)]
87. Manasa, P.; Sambasivam, S.; Ean, F. Recent progress on biomass waste derived activated carbon electrode materials for supercapacitors applications—A review. *J. Energy Storage* **2022**, *54*, 105290. [[CrossRef](#)]

**Disclaimer/Publisher’s Note:** The statements, opinions and data contained in all publications are solely those of the individual author(s) and contributor(s) and not of MDPI and/or the editor(s). MDPI and/or the editor(s) disclaim responsibility for any injury to people or property resulting from any ideas, methods, instructions or products referred to in the content.